THE ASTROPHYSICAL JOURNAL, 314:493–506, 1987 March 15

A SURVEY OF THE BOOTES VOID[1]

ROBERT P. KIRSHNER[2]
Harvard-Smithsonian Center for Astrophysics
AUGUSTUS OEMLER, JR.[2]
Yale University Observatory
AND
PAUL L. SCHECHTER[2] AND STEPHEN A. SHECTMAN[2]
Mount Wilson and Las Campanas Observatories
Received 1986 June 18; accepted 1986 September 2

ABSTRACT

In an earlier paper we inferred, from the distribution of galaxy redshifts in three small fields ~30° apart, the existence of a 10^6 Mpc^3 void in the distribution of galaxies in the constellation of Bootes. In this paper, we describe a redshift survey undertaken to test that hypothesis. Galaxies were selected by eye from 283 small fields distributed between the three original fields, and redshifts were measured for 239 of them. We confirm the existence of a large, roughly spherical void, of radius 62 Mpc, centered at $\alpha = 14^h50$, $\delta = +46°$, $v = 15{,}500$ km s^{-1}. The low density of this region is of high statistical significance and does not appear easily reconcilable with any of the popular models for the growth of structure in the universe. This void does contain some unusual galaxies characterized by strong, high-excitation emission spectra, but not in sufficient numbers to compensate for the absence of more usual objects.

Subject headings: galaxies: clustering — galaxies: redshifts

I. INTRODUCTION

While conducting a deep survey of the distribution of galaxies in six small, well-separated fields in the two Galactic caps (Kirshner *et al.* 1983*a*, hereafter KOSS), we discovered that the redshift distributions in each of the three northern fields showed an identical 6000 km s^{-1} gap (Kirshner *et al.* 1981). Because these fields were separated by angles of ~35°, this suggested the existence of a large void in the galaxy distribution of at least comparable angular diameter. Located in the constellation Bootes, this proposed feature has come to be called the Bootes Void.

At a mean recessional velocity of 15,000 km s^{-1}, this void would have a volume greater than 10^6 Mpc^3. Such a large void, if proved to be real, would put serious constraints on theories of the growth of structure in the universe, and it has been the subject of much theoretical speculation. Our hypothesis was, however, an extrapolation from limited data, and a much more extensive survey of the Bootes region was clearly needed to establish the reality of the void and delineate its structure. We have been engaged for some time on such a survey. While we have made a few preliminary reports (Kirshner *et al.* 1983*b*, 1984), the full results of our survey are presented in this paper.

In § II we describe the sample of galaxies chosen for study. In § III we present the results of a redshift survey of this sample, which confirms the reality of the void. Finally, in § IV we discuss the theoretical implications of this structure and its possible contents.

[1] Observations reported here were made in part at the Palomar Observatory as part of a collaborative agreement between the California Institute of Technology and the Carnegie Institution of Washington.

[2] Visiting Astronomer, Kitt Peak National Observatory, National Optical Astronomy Observatories, which is operated by the Association of Universities for Research in Astronomy, Inc., under contract with the National Science Foundation.

II. OBSERVATIONS

The size and distance of the Bootes Void make a complete redshift survey of its environs an impossibly large task. Therefore, in order to sample the distribution of galaxies, 283 small fields were chosen on a grid covering the region. Each field is a square 15′ on a side, and together they cover ~2% of the total area over which they are spread. The positions of the fields are given in Table 1, and their distribution on the sky is presented in Figure 1. Their unusual distribution is due to their having been chosen in three sets, each of the latter two sets being intended to refine the void outline detected in observations of the previous set.

Uniform enlargements of the fields were made from the Kitt Peak National Observatory's set of glass copies of the red plates of the Palomar Observatory Sky Survey, and copies of these photographs were distributed to the four authors. Each of us independently ranked, by eye, the brightness of all galaxies in the fields down to a limiting magnitude sufficient to give an average of about two galaxies per field. Galaxies were assigned a numerical rank, running from 1 for the brightest to *n* for the *n*th brightest. If the rankings were perfect, this set of galaxies, down to any rank, would comprise a perfect apparent magnitude–limited sample. Since our rankings were not perfect, or even consistent, we have averaged the four sets by the following technique.

If a galaxy was ranked by all four of us, a simple logarithmic mean of the four ranks was taken. However a galaxy was sometimes missing from one or more of the four ranked lists, either because it had been judged to be fainter than the cutoff brightness, or because it had been overlooked, or mistaken for a star. If the appearance or brightness of the galaxy suggested the latter case was true, the galaxy was assigned a rank equal to the mean of its logarithmic ranks on those lists on which it was included. If not, it was assumed to have an rank on the lists from which it was missing fainter than the cutoff and was

TABLE 1

SURVEY FIELDS

Field	R.A. (1950)	Dec (1950)	V_{lim}
1	13 38 36	+29 24 00	16.87
2	13 50 6	+29 24 00	16.87
3	14 1 36	+29 24 00	16.87
201	13 45 6	+30 39 00	16.87
202	13 56 42	+30 39 00	16.87
203	14 8 24	+30 39 00	16.87
204	14 20 0	+30 39 00	16.87
205	14 31 36	+30 39 00	16.87
206	14 43 12	+30 39 00	16.87
4	13 40 0	+31 54 00	16.87
5	13 51 48	+31 54 00	16.87
6	14 3 36	+31 54 00	16.87
7	14 15 18	+31 54 00	16.87
8	14 27 6	+31 54 00	16.87
207	13 46 42	+33 9 00	16.87
208	13 58 36	+33 9 00	16.87
209	14 10 36	+33 9 00	16.87
210	14 22 30	+33 9 00	16.87
211	14 34 24	+33 9 00	16.87
212	14 46 24	+33 9 00	16.87
213	14 58 18	+33 9 00	16.87
214	15 10 18	+33 9 00	16.87
9	13 41 24	+34 24 00	16.87
10	13 53 30	+34 24 00	16.87
11	14 5 36	+34 24 00	16.87
12	14 17 48	+34 24 00	16.87
13	14 29 54	+34 24 00	16.87
14	14 42 0	+34 24 00	16.87
15	14 54 6	+34 24 00	16.87
215	13 48 18	+35 39 00	16.87
216	14 0 36	+35 39 00	16.87
217	14 12 54	+35 39 00	16.87
218	14 25 12	+35 39 00	16.87
219	14 37 30	+35 39 00	16.87
220	14 49 48	+35 39 00	16.87
221	15 2 6	+35 39 00	16.87
222	15 14 24	+35 39 00	16.87
223	15 26 42	+35 39 00	16.87
16	13 42 48	+36 54 00	16.87
17	13 55 18	+36 54 00	16.87
18	14 7 48	+36 54 00	16.87
19	14 20 18	+36 54 00	16.87
20	14 32 48	+36 54 00	16.87
21	14 45 18	+36 54 00	16.87
22	14 57 48	+36 54 00	16.87
23	15 10 18	+36 54 00	16.87
24	15 22 48	+36 54 00	16.87
224	13 49 54	+38 9 00	16.87
225	14 2 36	+38 9 00	16.87
226	14 15 18	+38 9 00	16.87
227	14 28 0	+38 9 00	16.87
228	14 40 42	+38 9 00	16.87
229	14 53 24	+38 9 00	16.87
230	15 6 12	+38 9 00	16.87
231	15 18 54	+38 9 00	16.87
232	15 31 36	+38 9 00	16.87
233	15 44 18	+38 9 00	16.87
234	15 57 0	+38 9 00	16.87
25	13 44 12	+39 24 00	16.87
26	13 57 6	+39 24 00	16.37
27	14 10 6	+39 24 00	16.37
28	14 23 0	+39 24 00	17.19
302	14 29 30	+39 24 00	17.19
29	14 36 0	+39 24 00	17.19
303	14 42 24	+39 24 00	17.19
30	14 48 54	+39 24 00	16.87
304	14 55 24	+39 24 00	16.87
31	15 1 48	+39 24 00	16.87
305	15 8 18	+39 24 00	16.87
32	15 14 48	+39 24 00	16.87
33	15 27 42	+39 24 00	16.87
34	15 40 42	+39 24 00	16.87
235	13 51 30	+40 39 00	16.37
236	14 4 42	+40 39 00	16.37
237	14 17 54	+40 39 00	16.37
306	14 24 24	+40 39 00	17.19
238	14 31 0	+40 39 00	17.19
307	14 37 36	+40 39 00	17.19
239	14 44 12	+40 39 00	17.19
308	14 50 48	+40 39 00	16.87
240	14 57 24	+40 39 00	16.87
309	15 4 0	+40 39 00	16.87
241	15 10 36	+40 39 00	16.87
310	15 17 12	+40 39 00	16.87
242	15 23 48	+40 39 00	16.87
243	15 36 54	+40 39 00	16.87
244	15 50 6	+40 39 00	16.87
245	16 3 18	+40 39 00	16.87
246	16 16 30	+40 39 00	16.87
247	16 29 42	+40 39 00	16.87
35	13 45 36	+41 54 00	16.87
36	13 59 0	+41 54 00	16.37
37	14 12 30	+41 54 00	16.37
311	14 19 12	+41 54 00	16.87
38	14 25 54	+41 54 00	17.19
312	14 32 36	+41 54 00	17.19
39	14 39 18	+41 54 00	17.19
313	14 46 6	+41 54 00	17.19
40	14 52 48	+41 54 00	16.87
314	14 59 30	+41 54 00	16.87
41	15 6 12	+41 54 00	16.87
315	15 12 54	+41 54 00	16.87
42	15 19 36	+41 54 00	16.87
316	15 26 24	+41 54 00	16.87
43	15 33 6	+41 54 00	16.87
44	15 46 30	+41 54 00	16.87
45	16 0 0	+41 54 00	16.87
101	16 13 24	+41 54 00	16.87
102	16 26 48	+41 54 00	16.87
248	13 53 12	+43 9 00	16.37
249	14 6 54	+43 9 00	16.37
317	14 13 42	+43 9 00	16.37
250	14 20 36	+43 9 00	17.19
318	14 27 24	+43 9 00	17.19
251	14 34 18	+43 9 00	17.19
319	14 41 6	+43 9 00	17.19
252	14 48 0	+43 9 00	16.87
320	14 54 48	+43 9 00	16.87
253	15 1 42	+43 9 00	16.87
321	15 8 30	+43 9 00	16.87
254	15 15 24	+43 9 00	16.87
322	15 22 12	+43 9 00	16.87
255	15 29 6	+43 9 00	16.87
256	15 42 48	+43 9 00	16.87
257	15 56 30	+43 9 00	16.87
46	13 47 0	+44 24 00	16.87
47	14 1 0	+44 24 00	16.37
323	14 8 0	+44 24 00	16.87
48	14 15 0	+44 24 00	16.37
324	14 22 0	+44 24 00	16.87
49	14 28 60	+44 24 00	17.19
325	14 36 0	+44 24 00	16.87
50	14 43 60	+44 24 00	17.19
326	14 50 0	+44 24 00	16.87
51	14 57 0	+44 24 00	16.87
327	15 4 0	+44 24 00	16.87
52	15 11 0	+44 24 00	16.87
328	15 18 0	+44 24 00	16.87
53	15 25 0	+44 24 00	16.87
329	15 32 0	+44 24 00	16.87
54	15 39 0	+44 24 00	16.87
55	15 53 0	+44 24 00	16.87
103	16 7 0	+44 24 00	16.87
104	16 21 0	+44 24 00	16.87
258	13 54 54	+45 39 00	16.87
259	14 9 12	+45 39 00	16.87
330	14 16 18	+45 39 00	16.87
260	14 23 30	+45 39 00	16.87
331	14 30 36	+45 39 00	16.87
261	14 37 48	+45 39 00	16.87

TABLE 1—*Continued*

Field	R.A.(1950)	Dec(1950)	V_{lim}	Field	R.A.(1950)	Dec(1950)	V_{lim}
332	14 44 54	+45 39 00	16.87	74	14 23 36	+51 54 00	16.87
262	14 52 6	+45 39 00	16.87	359	14 31 42	+51 54 00	16.87
333	14 59 12	+45 39 00	16.87	75	14 39 48	+51 54 00	16.87
263	15 6 24	+45 39 00	16.87	360	14 47 54	+51 54 00	16.87
334	15 13 30	+45 39 00	16.87	76	14 56 0	+51 54 00	16.87
264	15 20 42	+45 39 00	16.87	361	15 4 6	+51 54 00	16.87
335	15 27 48	+45 39 00	16.87	77	15 12 12	+51 54 00	16.87
265	15 35 0	+45 39 00	16.87	362	15 20 18	+51 54 00	16.87
266	15 49 18	+45 39 00	16.87	109	15 28 24	+51 54 00	16.87
56	13 48 24	+46 54 00	16.87	110	15 44 36	+51 54 00	16.87
57	14 3 0	+46 54 00	16.87	280	14 0 12	+53 9 00	16.87
336	14 10 24	+46 54 00	16.87	281	14 16 54	+53 9 00	16.87
58	14 17 42	+46 54 00	16.87	282	14 33 36	+53 9 00	16.87
337	14 25 0	+46 54 00	16.87	363	14 41 54	+53 9 00	16.87
59	14 32 18	+46 54 00	16.87	283	14 50 18	+53 9 00	16.87
338	14 39 36	+46 54 00	16.87	364	14 58 36	+53 9 00	16.87
60	14 46 54	+46 54 00	16.87	284	15 6 54	+53 9 00	16.87
339	14 54 18	+46 54 00	16.87	78	13 52 36	+54 24 00	16.87
61	15 1 36	+46 54 00	16.87	79	14 9 48	+54 24 00	16.87
340	15 8 54	+46 54 00	16.87	80	14 27 0	+54 24 00	16.87
62	15 16 12	+46 54 00	16.87	81	14 44 6	+54 24 00	16.87
341	15 23 30	+46 54 00	16.87	82	15 1 18	+54 24 00	16.87
63	15 30 48	+46 54 00	16.87	111	15 18 30	+54 24 00	16.87
64	15 45 30	+46 54 00	16.87	112	15 35 42	+54 24 00	16.87
105	16 0 6	+46 54 00	16.87	285	14 2 12	+55 39 00	16.87
106	16 14 48	+46 54 00	16.87	286	14 19 54	+55 39 00	16.87
267	13 56 36	+48 9 00	16.87	287	14 37 36	+55 39 00	16.87
268	14 11 36	+48 9 00	16.87	288	14 55 18	+55 39 00	16.87
342	14 19 6	+48 9 00	16.87	83	13 54 0	+56 54 00	16.87
269	14 26 36	+48 9 00	16.87	84	14 12 18	+56 54 00	16.87
343	14 34 6	+48 9 00	16.87	85	14 30 36	+56 54 00	16.87
270	14 41 36	+48 9 00	16.87	86	14 48 54	+56 54 00	16.87
344	14 49 6	+48 9 00	16.87	113	15 7 12	+56 54 00	16.87
271	14 56 30	+48 9 00	16.87	114	15 25 36	+56 54 00	16.87
345	15 4 0	+48 9 00	16.87	289	14 4 12	+58 9 00	16.87
272	15 11 30	+48 9 00	16.87	290	14 23 6	+58 9 00	16.87
346	15 19 0	+48 9 00	16.87	291	14 42 6	+58 9 00	16.87
273	15 26 30	+48 9 00	16.87	87	13 55 24	+59 24 00	16.87
347	15 34 0	+48 9 00	16.87	88	14 15 0	+59 24 00	16.87
65	13 49 48	+49 24 00	16.87	89	14 34 42	+59 24 00	16.87
66	14 5 12	+49 24 00	16.87	90	14 54 18	+59 24 00	16.87
348	14 12 54	+49 24 00	16.87	115	15 14 0	+59 24 00	16.87
67	14 20 30	+49 24 00	16.87	116	15 33 36	+59 24 00	16.87
349	14 28 12	+49 24 00	16.87	292	14 6 18	+60 39 00	16.87
68	14 35 54	+49 24 00	16.87	293	14 26 42	+60 39 00	16.87
350	14 43 36	+49 24 00	16.87	294	14 47 6	+60 39 00	16.87
69	14 51 18	+49 24 00	16.87	91	13 56 48	+61 54 00	16.87
351	14 59 0	+49 24 00	16.87	92	14 18 0	+61 54 00	16.87
70	15 6 36	+49 24 00	16.87	93	14 39 18	+61 54 00	16.87
352	15 14 18	+49 24 00	16.87	117	15 0 30	+61 54 00	16.87
71	15 22 0	+49 24 00	16.87	118	15 21 42	+61 54 00	16.87
353	15 29 42	+49 24 00	16.87	295	14 8 36	+63 9 00	16.87
107	15 37 24	+49 24 00	16.87	296	14 30 42	+63 9 00	17.34
108	15 52 42	+49 24 00	16.87	94	13 58 12	+64 24 00	16.87
274	13 58 24	+50 39 00	16.87	95	14 21 18	+64 24 00	17.34
275	14 14 12	+50 39 00	16.87	119	14 44 30	+64 24 00	17.34
354	14 22 0	+50 39 00	16.87	120	15 7 36	+64 24 00	17.34
276	14 29 54	+50 39 00	16.87	297	14 11 0	+65 39 00	16.87
355	14 37 48	+50 39 00	16.87	96	13 59 36	+66 54 00	16.87
277	14 45 42	+50 39 00	16.87	97	14 25 6	+66 54 00	17.34
356	14 53 36	+50 39 00	16.87	121	14 50 36	+66 54 00	16.87
278	15 1 30	+50 39 00	16.87	122	15 16 6	+66 54 00	16.87
357	15 9 24	+50 39 00	16.87	298	14 13 42	+68 9 00	16.87
279	15 17 12	+50 39 00	16.87	98	14 1 0	+69 24 00	16.87
358	15 25 6	+50 39 00	16.87	123	14 29 24	+69 24 00	16.87
72	13 51 12	+51 54 00	16.87	124	14 57 48	+69 24 00	16.87
73	14 7 24	+51 54 00	16.87				

assigned a best-guess rank on each of these lists. This best guess was found by an iterative technique. Assigning to the galaxy a tentative rank equal to the mean of the available ranks, and assuming a ranking error with a normal distribution of standard deviation 0.3 in the natural log of the rank, we calculate the probability $P(R)$ that one of us would have given the galaxy a particular rank R. This $P(R)$ is zero for R less than the cutoff rank and has a monotonically decreasing positive value for all larger ranks. The most probable rank is the center of gravity of the distribution of $P(r)$. We take this rank, average it with the other available ranks for the galaxy, and iterate until this average converges. This value we take as the final estimate of the galaxy's rank.

To calibrate our rankings and estimate their accuracy, photoelectric photometry in the J and F bands (see Kirshner, Oemler, and Schechter 1978) was obtained for 59 of the galaxies using the Mark 2 photometer on the KPNO 1.3 m telescope. The apertures used were large enough (typically 36″) to

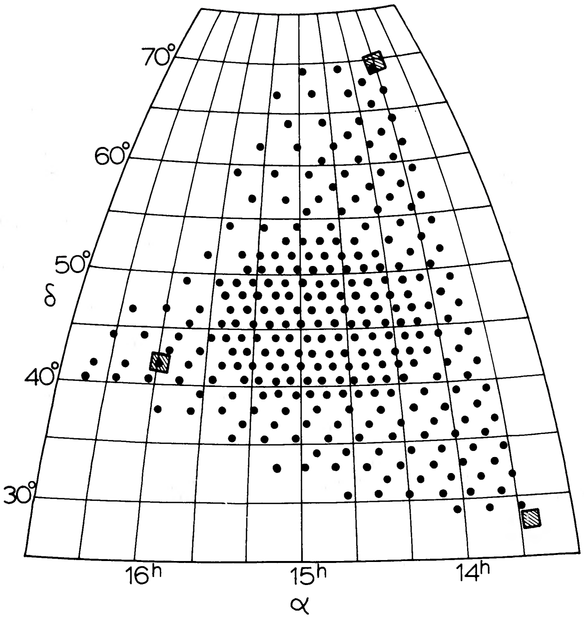

FIG. 1.—Distribution of survey fields (dots not to scale). The shaded squares are the three northern KOSS fields.

contain almost all the light of all but the few brightest galaxies. A plot of galaxy rank versus photoelectric F-magnitude should be exactly equivalent to the galaxy number count versus magnitude relation for this region of the sky, with the addition of three sources of error: a scatter of order the square root of the rank due to the random sampling of the galaxy population, and scatter due to errors in the photoelectric photometry and the eye rankings. While this is basically true of our data, the residuals from the mean rank–magnitude relation show two systematic trends.

First, they are a systematic function of galaxy color, redder galaxies being ranked too low (faint). The probable reason is that red galaxies tend to be of higher surface brightness than blue galaxies; their images are more saturated and appear relatively fainter. The result is that our eyeball photometry is effectively in a band to the blue of the F band by an amount

$$\Delta m = 0.66(J - F) . \quad (1)$$

By coincidence, this shift is almost exactly that between the V and F bands (Kirshner, Oemler, and Schechter 1978), so that our ranked list actually best approximates a V-magnitude–limited sample.

The second systematic trend is a correlation of the residuals with the POSS field in which the galaxies lie, indicating a (not unexpected) field-to-field variation in the depth of the POSS plates. Of the 22 POSS fields in which we have calibrations, five appear to differ significantly from the mean, by amounts of up to 0.6 mag. These differences in field depth have been taken into account in the final calibration. Unfortunately, there are nine POSS fields, containing 27 of our 283 survey fields, for which we do not have calibrations. Extrapolating from the calibrated fields, we might expect about two of these to have significantly different zero points, producing an unaccounted-for variation in the depth of roughly 2% of our survey.

The final rank–V-magnitude relation, including color and field corrections, is presented in Figure 2. The fractional rank R is defined so that the 283d galaxy has a rank of 1.00. The filled circles are the galaxies with photoelectric photometry; the error bars are 1 σ uncertainties in the latter. The open circles are galaxies in KOSS field NP 8 with photographic photometry. Galaxies in this field were included in the ranking process as an independent calibration, and their position in Figure 2 confirms the zero point derived from the photoelectric photometry. The solid line is a best fit to the data and follows the equation

$$V = 16.98 + 1.94 \log R + \Delta , \quad (2)$$

where Δ is a correction applied to galaxies in the five POSS fields which differ significantly from the others. The scatter in the true V-magnitudes about the values predicted by equation (2) has a standard deviation of 0.29 mag, sufficiently small for our purposes—indeed, gratifyingly small considering our photometric technique. A list of the brighest 300 galaxies is presented in Table 2.

We have measured redshifts of 231 galaxies from Table 2, using the SIT and intensified reticon scanner on the Palomar 5 m telescope and the IIDS on the KPNO 2.1 m telescope. Values of cz, which we shall for convenience call velocities, corrected to the rest frame of the Local Group according to the precepts of de Vaucouleurs, de Vaucouleurs, and Corwin (1976, hereafter RC2), are presented in the fifth column of Table 2. We estimate these velocities to be accurate to ~ 100 km s^{-1} (1 standard deviation). Velocities for eight galaxies, taken from RC2 and from the CfA survey (Huchra *et al.* 1983) are also included.

The velocity measurements are 97% complete to a fractional rank $R = 0.82$; fainter than this the completeness factor is very low. Therefore we take this as the limit of what we shall call the nearly complete sample. Since the missing brighter galaxies are scattered rather uniformly throughout the rankings, this is a

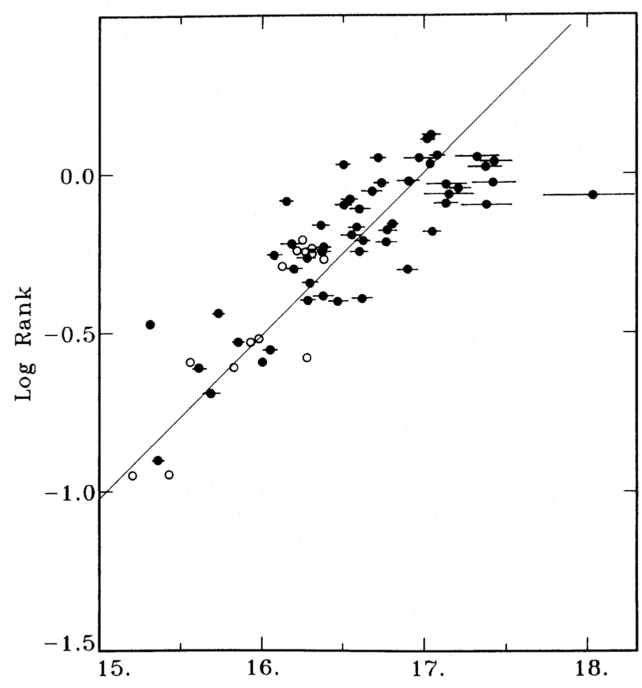

FIG. 2.—V-magnitudes of galaxies vs. their estimated rank. *Filled circles*, galaxies in this sample with photoelectric photometry; *open circles*, galaxies from NP 8 with photographic photometry from KOSS.

1987ApJ...314..493K

TABLE 2

THE GALAXY SAMPLE

R.A. (1950)	Dec (1950)	Field	Rank	cz
13 51 13	+40 36 42	235	0.007	2410[a]
15 19 26	+41 54 30	42	0.008	5720[b]
13 51 18	+40 33 0	235	0.010	3100[b]
13 40 18	+31 47 0	4	0.018	7710
13 51 18	+40 31 54	235	0.019	2260[a]
14 51 52	+49 20 36	69	0.025	9350
13 45 5	+30 35 6	201	0.027	4600
13 49 43	+29 18 24	2	0.028	11300
13 51 37	+40 35 0	235	0.029	2460[a]
14 21 56	+33 16 12	210	0.036	1790[a]
14 29 28	+39 28 48	302	0.036	7160
14 34 38	+59 27 42	89	0.041	20700
13 50 23	+38 4 0	224	0.045	3740[a]
13 48 7	+35 43 12	215	0.051	7950
15 10 34	+40 44 6	241	0.057	9490
13 53 7	+34 25 12	10	0.062	19400
14 43 18	+30 37 54	206	0.063	8870
13 54 3	+34 27 54	10	0.064	10280
13 57 23	+61 55 12	91	0.067	9240
14 49 13	+35 45 0	220	0.074	1360[a]
15 10 0	+33 6 0	214	0.080	6980
15 18 1	+44 29 48	328	0.081	8660
14 39 3	+41 50 48	39	0.085	5770
14 17 34	+40 33 48	237	0.090	7760
14 18 7	+34 28 24	12	0.090	20430
15 8 3	+64 22 0	120	0.091	13220
14 19 30	+48 9 0	342	0.093	22090
15 10 4	+36 50 18	23	0.096	19810
14 6 36	+60 34 12	292	0.100	11330
13 56 36	+61 57 24	91	0.102	21230
14 18 7	+34 23 48	12	0.105	20580
13 54 10	+56 49 18	83	0.109	21180
14 53 33	+50 42 6	356	0.111	11450
14 46 31	+41 50 48	313	0.113	5600
14 18 11	+34 26 48	12	0.117	20360
14 40 48	+38 5 0	228	0.120	9640
14 43 35	+49 20 30	350	0.126	11270
14 1 6	+35 33 48	216	0.127	14440
14 10 55	+48 14 48	268	0.130	
15 10 24	+40 37 0	241	0.133	9790
13 54 0	+34 29 0	10	0.135	10480
14 59 11	+49 21 6	351	0.136	9650
14 15 45	+45 41 30	330	0.139	8390
14 9 33	+39 23 0	27	0.143	13320
15 6 58	+56 51 54	113	0.145	8970
14 58 54	+49 22 6	351	0.161	9290
14 50 55	+53 13 18	283	0.165	19450
14 45 0	+64 18 54	119	0.166	34580
13 44 40	+39 20 12	25	0.172	18530
14 19 40	+48 11 24	342	0.174	21000
13 57 6	+30 39 54	202	0.184	14120
14 5 19	+49 19 42	66	0.185	21440
13 48 36	+35 42 6	215	0.186	
14 51 45	+49 18 48	69	0.202	11070
15 18 39	+48 11 30	346	0.202	23690
13 57 5	+30 41 6	202	0.205	14780
14 32 36	+46 48 0	59	0.207	10710
15 17 28	+50 43 0	279	0.210	11630
13 43 19	+36 48 42	16	0.223	18490
13 52 48	+54 22 0	78	0.224	21000
14 2 58	+55 40 18	285	0.228	1610
13 44 40	+30 37 12	201	0.229	35280
14 23 38	+51 47 6	74	0.234	2070
15 24 46	+57 0 6	114	0.235	15700
14 39 25	+62 0 42	93	0.237	14600
14 22 6	+44 27 36	324	0.240	18700
14 59 12	+53 13 54	364	0.245	23010
14 14 5	+50 33 36	275	0.246	22320
15 8 28	+64 17 24	120	0.250	22780
14 22 36	+39 26 0	28	0.250	26540
15 41 18	+39 18 36	34	0.251	19290
14 14 23	+59 20 0	88	0.253	22460
14 16 58	+45 35 12	330	0.257	8450
14 57 11	+48 13 12	271	0.257	
14 19 34	+30 45 48	204	0.257	20440
14 8 37	+45 45 54	259	0.264	10840
15 17 19	+40 41 18	310	0.266	27050
15 14 28	+35 36 54	222	0.269	19940
14 29 6	+69 21 54	123	0.270	33810
15 11 6	+40 43 24	241	0.270	8990
14 22 18	+33 10 36	210	0.273	2270
15 14 18	+35 36 0	222	0.275	20150
14 51 36	+49 24 6	69	0.279	19880
14 10 13	+39 31 6	27	0.280	7870
13 54 48	+36 47 24	17	0.294	18530
14 39 51	+46 48 0	338	0.296	25460
14 18 11	+40 34 54	237	0.300	7680
15 14 53	+43 7 54	254	0.307	5500
14 12 21	+35 36 24	217	0.309	17510
15 59 28	+42 0 54	45	0.309	7320
14 12 36	+49 22 0	348	0.316	21500
15 13 12	+41 54 24	315	0.322	19800
14 12 19	+35 45 36	217	0.324	4110
15 46 34	+41 55 54	44	0.325	10060
13 53 7	+34 21 24	10	0.330	19170
15 49 13	+45 39 54	266	0.334	17670
14 39 53	+46 48 48	338	0.336	29690
14 11 10	+48 9 0	268	0.336	18050
15 15 44	+66 51 36	122	0.344	17370
14 49 3	+56 47 24	86	0.344	23740
15 27 19	+39 27 24	33	0.350	19660
14 0 2	+35 40 12	216	0.357	10390
14 5 30	+49 21 30	66	0.357	24900
13 53 1	+43 11 24	248	0.361	19500
14 10 52	+48 11 36	268	0.363	20950
14 3 2	+38 4 48	225	0.365	19710
14 38 40	+61 51 0	93	0.368	14660
15 26 16	+56 49 18	114	0.368	11980
13 38 51	+29 20 30	1	0.370	34960
14 1 3	+35 35 6	216	0.371	14900
14 11 51	+48 11 6	268	0.378	21000
15 10 0	+36 58 18	23	0.380	13510
14 40 10	+38 4 54	228	0.382	
14 58 34	+53 9 6	364	0.384	22760
14 43 24	+49 18 48	350	0.386	
13 53 43	+56 53 18	83	0.389	13480
13 53 4	+43 10 54	248	0.389	19200
14 50 40	+49 22 24	69	0.398	22860
14 41 33	+34 25 48	14	0.400	36340
14 12 36	+35 36 48	217	0.401	17810
13 56 12	+30 35 0	202	0.401	18780
14 12 56	+35 45 48	217	0.406	20280
15 10 59	+48 4 30	272	0.410	21650
14 37 43	+45 44 0	261	0.416	37930
14 44 3	+64 21 24	119	0.417	34860
15 19 55	+41 51 0	42	0.418	40420
15 28 3	+45 37 0	335	0.424	21520
14 10 24	+39 29 0	27	0.432	7580
13 56 43	+30 41 54	202	0.432	21050
15 15 37	+46 53 36	62	0.438	6230
15 16 29	+66 48 48	122	0.442	17060
15 33 25	+59 17 6	116	0.449	29630
15 22 2	+61 55 6	118	0.452	32390
15 15 37	+43 8 6	254	0.456	5550
15 16 15	+66 50 36	122	0.459	17030
14 52 0	+49 30 36	69	0.460	51410
14 45 21	+64 17 54	119	0.460	17630
14 38 51	+61 50 18	93	0.462	14610
15 8 8	+64 24 18	120	0.463	22630
15 18 55	+54 18 36	111	0.473	48520
13 53 45	+56 51 54	83	0.486	29470
14 33 31	+48 13 6	343	0.498	33490
15 33 36	+42 0 12	43	0.498	24430
15 45 1	+46 59 54	64	0.504	20170
14 12 40	+35 37 30	217	0.507	17780
15 6 0	+49 27 54	70	0.508	32750
15 6 12	+45 32 24	263	0.508	28880
14 58 46	+49 26 54	351	0.516	4500
13 59 5	+33 1 54	208	0.517	14900
14 9 51	+54 27 48	79	0.524	22500

TABLE 2—*Continued*

R.A.(1950)	Dec(1950)	Field	Rank	cz
14 27 34	+49 26 12	349	0.528	21180
15 41 1	+39 24 24	34	0.529	18610
14 58 24	+49 27 36	351	0.531	8170
15 6 52	+45 40 6	263	0.536	26330
14 35 25	+39 20 0	29	0.537	29410
16 12 55	+41 50 6	101	0.540	8150
15 31 29	+38 7 54	232	0.541	4630
14 31 25	+63 10 54	296	0.546	20910
15 0 45	+54 27 48	82	0.550	43170
14 24 46	+40 37 54	306	0.559	25180
13 53 31	+43 2 54	248	0.560	19700
15 37 19	+49 27 48	107	0.565	22420
15 8 41	+39 20 54	305	0.566	18810
14 51 15	+66 47 0	121	0.569	34160
15 57 10	+38 3 0	234	0.574	36120
14 45 42	+50 40 36	277	0.574	9250
14 55 4	+39 20 6	304	0.574	8510
14 29 24	+34 21 24	13	0.574	38460
14 25 4	+46 50 54	337	0.575	8610
15 33 18	+41 52 48	43	0.578	35490
13 49 35	+38 6 0	224	0.580	19000
14 37 6	+55 45 0	287	0.581	29000
14 13 36	+49 22 12	348	0.582	21510
15 16 9	+66 47 30	122	0.582	17090
15 21 24	+62 0 30	118	0.583	22750
15 11 35	+48 2 54	272	0.591	8040
15 25 8	+56 55 12	114	0.592	33740
14 59 14	+41 52 36	314	0.595	28220
15 17 24	+40 43 30	310	0.599	26970
14 34 16	+48 13 54	343	0.605	34060
14 19 10	+48 15 54	342	0.611	20960
14 37 37	+55 45 24	287	0.612	37950
14 30 25	+34 19 36	13	0.612	12880
15 34 37	+45 35 18	265	0.617	22800
14 28 18	+49 26 36	349	0.618	11790
14 51 31	+49 28 12	69	0.619	22900
14 43 17	+30 45 30	206	0.620	33790
14 26 51	+31 49 0	8	0.633	36720
15 6 6	+49 18 42	70	0.647	34630
14 3 10	+46 47 18	57	0.650	20080
14 34 56	+33 13 18	211	0.657	3780
14 14 34	+59 19 48	88	0.660	22330
14 55 18	+43 9 36	320	0.670	34470
14 46 8	+42 0 12	313	0.671	39090
15 21 49	+61 57 54	118	0.677	23100
14 34 15	+59 28 30	89	0.682	20580
14 29 33	+44 29 12	49	0.690	46160
15 13 59	+35 33 6	222	0.695	16260
14 29 28	+44 25 54	49	0.696	
14 21 19	+64 18 48	95	0.697	32950
14 11 58	+41 49 42	37	0.698	12180
15 3 32	+51 58 0	361	0.700	29680
14 54 16	+43 10 6	320	0.708	33980
15 20 33	+45 40 48	264	0.711	18870
15 34 53	+45 34 54	265	0.714	22700
14 14 30	+59 19 0	88	0.715	22520
14 16 49	+53 7 6	281	0.715	24690
15 17 33	+50 38 30	279	0.716	22820
13 51 11	+40 33 48	235	0.717	2690
14 42 40	+30 42 36	206	0.717	18770
15 16 15	+66 48 0	122	0.722	
15 1 40	+35 35 6	221	0.728	19840
15 26 40	+35 36 48	223	0.729	44170
14 38 6	+55 39 24	287	0.736	22670
14 31 7	+51 50 54	359	0.753	42950
15 32 52	+59 20 54	116	0.757	17620
14 27 52	+43 9 36	318	0.767	2650
15 11 48	+48 8 48	272	0.768	35860
14 20 37	+36 52 12	19	0.778	22760
13 55 49	+36 56 42	17	0.784	42440
14 2 18	+69 25 6	98	0.786	9530
14 18 14	+34 26 0	12	0.792	20430
14 2 55	+38 4 18	225	0.797	19680
14 18 58	+48 13 6	342	0.797	
14 25 1	+46 57 36	337	0.802	22300
14 19 58	+55 33 54	286	0.806	38060
14 25 1	+46 52 48	337	0.813	22410
14 18 31	+40 34 12	237	0.815	25490
14 28 41	+49 26 30	349	0.816	11740
14 12 19	+41 56 24	37	0.818	24730
16 27 4	+41 55 12	102	0.823	
15 14 36	+49 20 36	352	0.825	
14 11 12	+48 7 12	268	0.827	
14 27 5	+43 7 12	318	0.829	37620
15 22 15	+61 52 48	118	0.831	32580
13 52 53	+54 19 48	78	0.835	21260
14 0 30	+44 21 24	47	0.836	36750
14 54 42	+43 14 18	320	0.837	
14 17 29	+53 5 48	281	0.840	
15 16 18	+66 49 18	122	0.842	
14 3 49	+58 11 0	289	0.845	
13 56 18	+59 25 54	87	0.845	11290
14 59 17	+53 2 12	364	0.847	23020
14 16 48	+53 7 48	281	0.847	
16 6 36	+44 17 6	103	0.851	15270
14 23 53	+51 57 42	74	0.852	11810
15 23 17	+46 54 36	341	0.857	
15 29 43	+43 10 18	255	0.858	
13 56 16	+30 34 36	202	0.865	
15 33 53	+48 9 18	347	0.868	
15 30 16	+49 22 48	353	0.869	
14 40 26	+51 52 42	75	0.870	38880
16 16 23	+40 43 48	246	0.870	
13 51 56	+54 25 30	78	0.871	29700
14 42 31	+34 29 0	14	0.877	38260
13 52 46	+43 3 0	248	0.882	
14 43 10	+30 45 48	206	0.890	
14 18 22	+61 47 30	92	0.894	
14 37 30	+55 34 6	287	0.896	
14 29 11	+69 30 36	123	0.898	15430
14 59 13	+41 57 48	314	0.911	
14 19 48	+36 50 36	19	0.924	29660
14 20 0	+30 43 42	204	0.935	
14 8 1	+30 32 12	203	0.940	
14 50 30	+53 10 48	283	0.945	
15 27 7	+45 32 30	335	0.949	
13 54 43	+36 50 0	17	0.955	18650
15 7 48	+56 50 48	113	0.957	
14 34 29	+33 6 48	211	0.964	
13 58 56	+33 4 54	208	0.968	
14 34 48	+43 12 0	251	0.973	
15 13 11	+41 47 42	315	0.976	
13 40 7	+31 58 36	4	0.978	
14 27 18	+43 14 36	318	0.985	
14 18 59	+41 59 12	311	0.988	
14 43 23	+49 28 30	350	0.989	
15 1 43	+35 40 36	221	0.990	
15 40 40	+39 25 12	34	0.993	31450
13 46 40	+44 30 48	46	0.994	
15 15 45	+46 54 12	62	0.994	
14 20 16	+49 28 18	67	0.999	
14 17 35	+40 42 0	237	1.000	
14 39 49	+51 52 12	75	1.005	
15 9 49	+36 57 18	23	1.033	13490
15 22 27	+61 52 48	118	1.036	31780
14 39 43	+46 53 6	338	1.036	
14 39 15	+47 1 0	338	1.036	
16 20 36	+44 25 24	104	1.044	
15 27 22	+45 44 48	335	1.045	
14 11 21	+48 10 6	268	1.055	
14 20 6	+30 33 48	204	1.060	
14 15 41	+38 5 48	226	1.061	
14 38 19	+61 53 12	93	1.061	
15 33 22	+42 0 54	43	1.065	
14 23 23	+45 37 36	331	1.067	
14 27 6	+43 15 0	255	1.073	
14 39 25	+51 53 30	75	1.077	
13 57 7	+30 34 12	202	1.082	
15 5 41	+41 56 42	41	1.082	
15 1 54	+43 14 36	253	1.083	

[a] From CfA survey.
[b] From RC2.

reasonable approach, provided that we divide all galaxy densities derived from this sample by 0.97. With a limiting rank of 0.82, and using equation (2), we calculate the limiting magnitude of the nearly complete velocity sample in each survey field; this quantity is presented in the last column of Table 1.

III. THE DISTRIBUTION OF GALAXIES

To convey the three-dimensional distribution of our galaxies, we present the data in several different ways. Each has limitations, but together they give a reasonably complete idea of the structure of the region we have surveyed. In Figure 3 we present the distribution of measured velocities of our galaxies. The nearly complete sample is represented by the shaded area, and the remaining galaxies by the open area. The smooth curve is the predicted distribution of the nearly complete sample in a homogeneous universe. If the luminosity function of galaxies is of the form (Schechter 1976)

$$\phi(L)dL = \phi^*(L/L^*)^{\alpha} e^{-L/L^*} \, dL/L^* \,, \tag{3}$$

then the space density of galaxies in a shell of distance R in an apparent magnitude–limited sample is

$$\rho(m_{\rm lim}, R) = \phi^*(R)\Gamma\{\alpha + 1, \text{dex} \times [0.4(M^* - m_{\rm lim} + 5 \log R - 5)]\} \,, \tag{4}$$

where M^* is the magnitude corresponding to L^* (see, e.g., Kirshner, Oemler, and Schechter 1979). The large photometry errors in our sample make it an imperfect approximation to a magnitude–limited sample. However, if the magnitude errors have a normal distribution, it is straightforward to

$$\rho(m_{\rm lim}, R) = \frac{\phi^*}{2}\left[\Gamma(\alpha + 1) - \int_0^{\infty} \text{erf}\left\{\frac{[M^* - m_{\rm lim} - 2.5 \log (L/L^*) + 5 \log R - 5]}{\sqrt{2\sigma^2}}\right\} \times e^{-(L/L^*)}\left(\frac{L}{L^*}\right)^{\alpha} d\left(\frac{L}{L^*}\right)\right] . \tag{5}$$

where σ is the standard deviation of the magnitude errors. We have used equation (5) with the values $\phi^* = 1.5 \times 10^{-3}$, $M_v^* = -22.0$, and $\alpha = -1.25$ derived in KOSS to calculate the expected density distribution.

In Figure 4 we present the distribution of galaxies in the velocity-declination plane, with three intervals of right ascension indicated by different symbols. In addition to the expected variation in the number of galaxies with velocity described by equation (5), it should be noted that the density of galaxies varies with declination because of a corresponding variation in the number of fields.

In Figure 5 we present a stereoscopic view of the sample, from the same viewpoint as in Figure 4. This figure may be viewed by placing an index card upright between the two plots and putting the bridge of the nose against its end. After some moments of eye adjustment, the reader will get either a headache or a stereo view of the Bootes region.

All the views described above suffer in one way or another from the variable density of sample fields across the sky or the variation in the sampling function with depth, or both. In

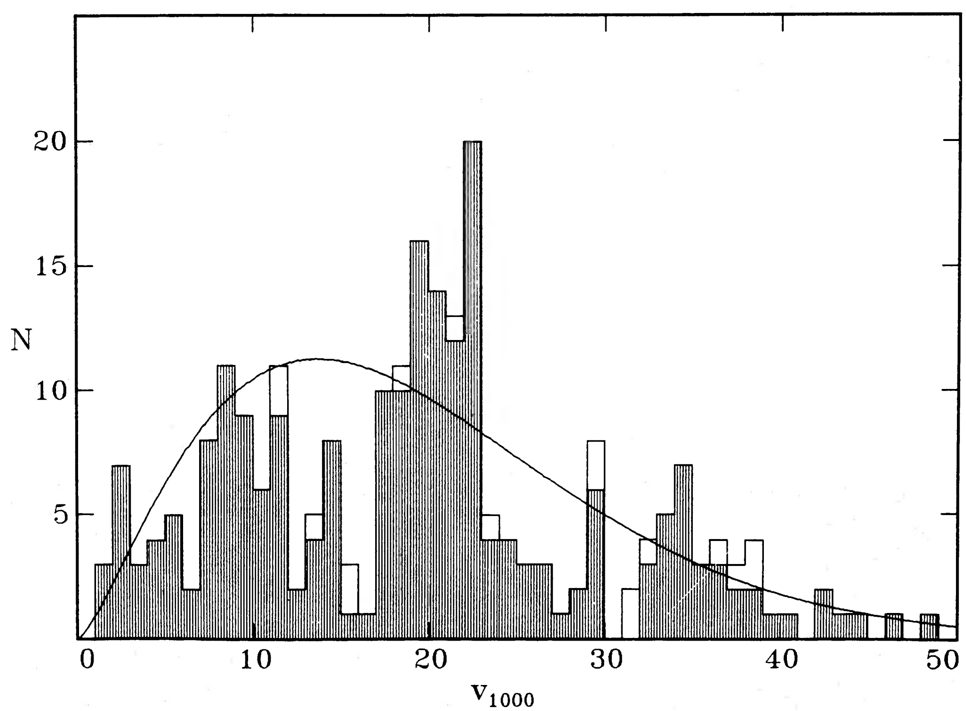

FIG. 3.—Distribution of velocities of the sample galaxies. *Shaded area*, nearly complete sample; *open area*, other galaxies; *smooth curve*, distribution expected in a homogeneous universe.

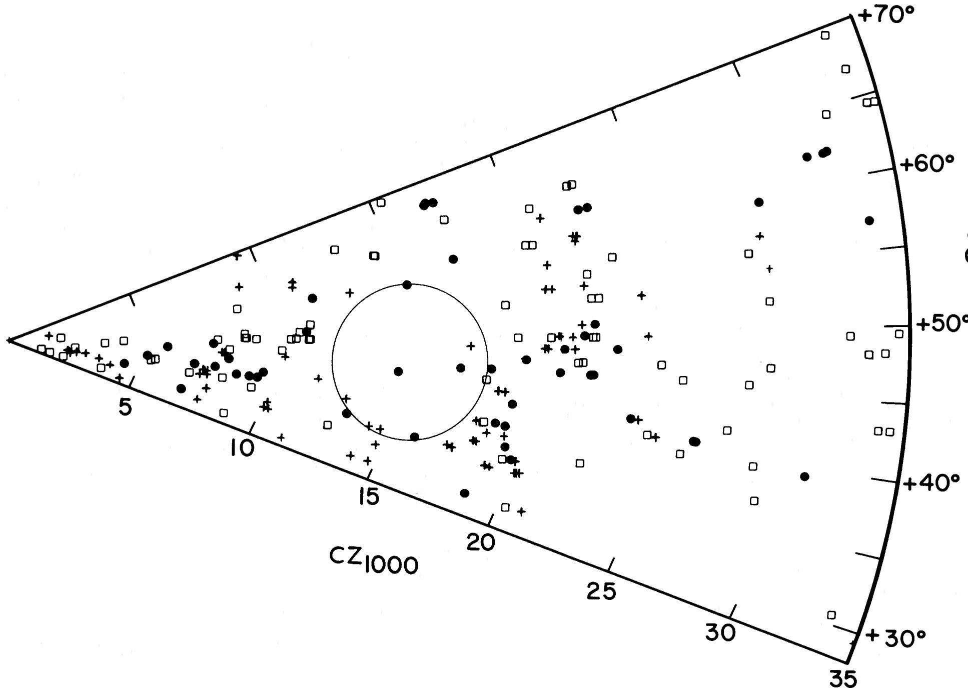

FIG. 4.—Distribution in the velocity-declination plane of sample galaxies. *Filled circles*, galaxies with $\alpha > 15^h10^m$; *open circles*, galaxies with $14^h20^m < \alpha \leq 15^h10^m$; *pluses*, galaxies with $\alpha \leq 14^h20^m$. The large circle represents the largest empty sphere that will fit within the void.

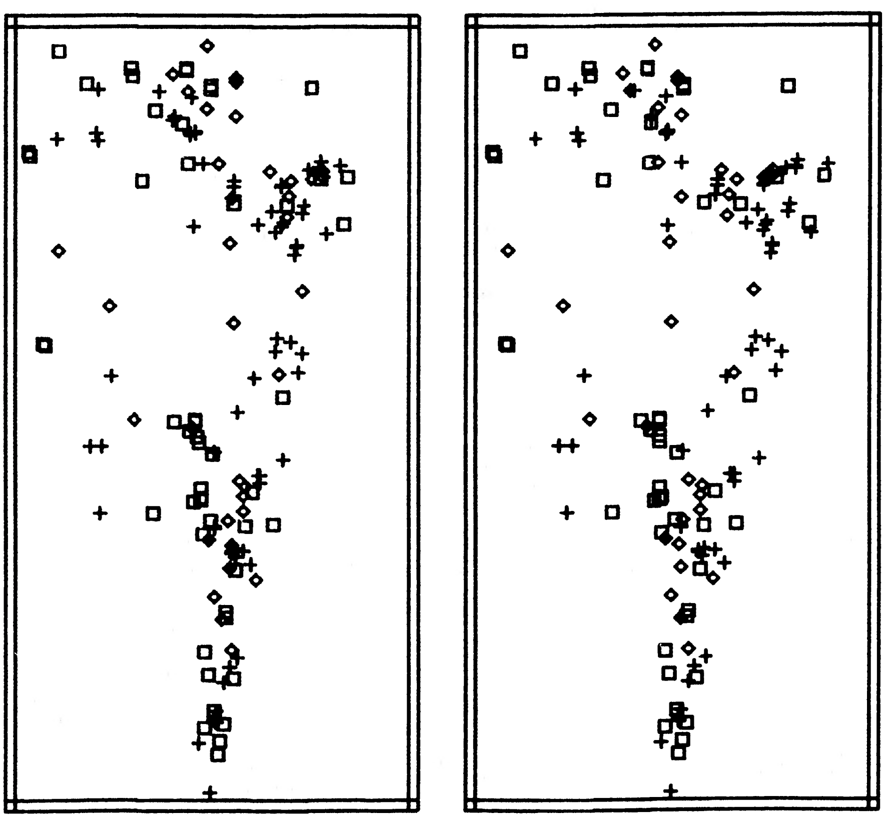

FIG. 5.—Stereoscopic view of the galaxy distribution, from the same viewpoint as Fig. 4

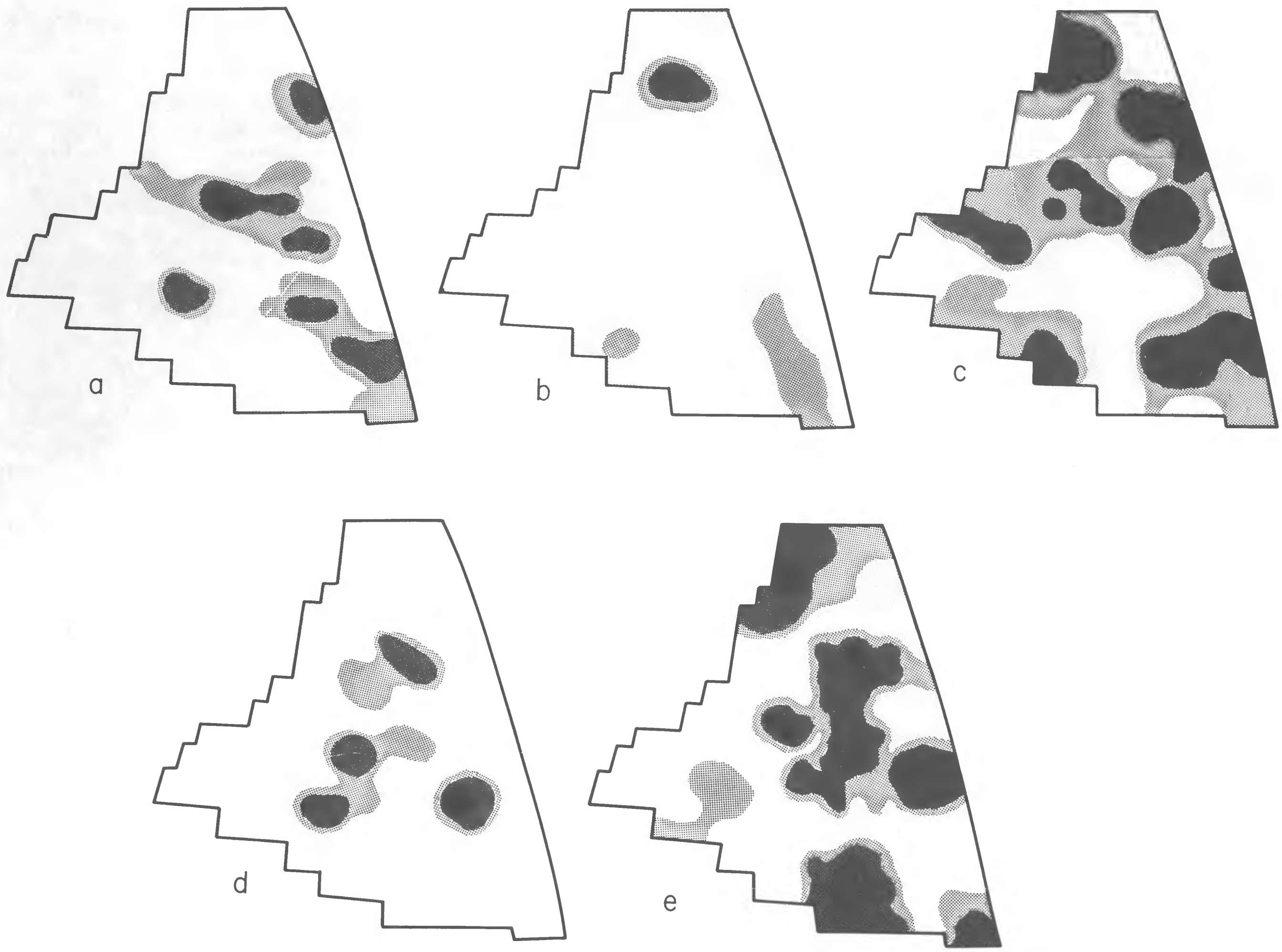

FIG. 6.—Contours of space density of galaxies in five velocity intervals. The lowest contour represents a density equal to 0.7 of the cosmic mean; each higher contour represents a factor of 2 increase in density. Velocity ranges (km s^{-1}): (*a*) 7000–12,000; (*b*) 12,000–17,000; (*c*) 17,000–23,000; (*d*) 23,000–29,000; (*e*) 29,000–39,000.

Figure 6 we correct for these effects, using the predicted variation in the sampling function with distance, calculated using equation (5) and the galaxy parameters from KOSS, and taking into account the variation in the density of sample fields across the sky. Figure 6 presents contours of the true space density of galaxies across our survey area, in five velocity intervals. To handle the discreteness of the sample fields, these contour plots have been smoothed at each point over an area containing the nearest five fields.

Inspection of Figures 3–6 reveals three major points. First, the distribution of galaxies is very inhomogeneous, with large density excesses near velocities of 10,000 and 20,000 km s^{-1} and a large deficit near 15,000 km s^{-1}. Second, unlike the velocity distribution in the three northern KOSS fields, the interval between 12,000 and 18,000 km s^{-1} is not completely empty. Nevertheless, there is a large void in this region. It is most apparent in Figure 6*b*, where it appears roughly circular in outline. Indeed, although the clumpy distribution of galaxies and the finite size of our velocity sample make it impossible to precisely determine its shape, the data are consistent with its being approximately spherical. The largest empty sphere which we can put into our sample has a radius of 63 Mpc (assuming $H_0 = 50$ km s^{-1} Mpc^{-1}) and is centered at $\alpha = 14^h50^m$, $\delta = +46°$, $cz = 15{,}500$ km s^{-1}. The location and size of this sphere is indicated by the circle in Figure 4. Its volume is 1.0×10^6 Mpc^3.

What is the statistical significance of this empty sphere? If our galaxies had the distribution shown by the smooth curve in Figure 3, the sphere should contain 31 galaxies. If their positions were uncorrelated, the chance of the sphere containing no galaxies when 31 were expected would be $\exp(-31) = 3.4 \times 10^{-14}$. However, this naive calculation ignores two important factors. One point is that, because galaxies are correlated, the number of independent points is less than 31. We calculate that number as follows. The distribution of separations between pairs of galaxies within single fields shows an excess at small separations over the number expected if galaxies were randomly distributed. About 80% of these excess pairs have velocity differences less than 500 km s^{-1} and almost all have velocity differences less than 1000 km s^{-1}. We now identify all pairs (including interfield pairs) with separations of less than $5h^{-1}$ or $10h^{-1}$ Mpc and recessional velocities $10{,}000 < v < 20{,}000$ km s^{-1} and use a friends-of-friends technique to build groups out of common pairs. Using a $5h^{-1}$ Mpc separation length, we find that the 71 galaxies in this velocity range fall into 50 groups; using $10h^{-1}$ Mpc they fall into 38 groups. We may then say that the ratio of independent groups to galaxies is $\sim 40/71$. Thus our 31 missing galaxies represent 17.5 independent groups. Since $\exp(-17.5) = 2.6 \times 10^{-8}$, the probability of a volume being empty is still very small. Using the same statistic, we calculate that there is a 1% chance that the density within the void is higher than one-quarter the cosmic mean.

However, as Politzer and Preskill (1986) have recently demonstrated, the probability of finding one such empty sphere of volume v somewhere within a larger volume V is much larger, typically by an factor of $(V/v)(17.5)^3$. Fortunately, our case is not typical, for two reasons. First, the volume over which we can search is not much larger than the void. Because the empty sphere subtends an angle almost as large as that of our survey region, we cannot move the sphere very far across the sky before touching the edge of our survey region. For the same reason, we cannot move it much closer. If we move it farther from us, on the other hand, the galaxy selection function decreases the density of sample galaxies so fast that the total number of expected galaxies does not increase even if we expand the size of the sphere to the limits of the survey area. Thus the spherical void is close to being the most improbable one that could exist within our survey volume.

Our case is also not typical because we sample the galaxy distribution in discrete fields. In the Appendix, we derive an expression for the void probability, analogous to equation (2) of Politzer and Preskill, which takes account of this difference in sampling. Applying this equation to our sample, we find that the probability of finding, somewhere within our survey volume, a void at least as large and as improbable as ours is larger than $\exp(-17.5)$ by a factor of only ~ 50. Thus, $P_{\rm void} \approx 10^{-6}$.

Our original claim for the existence of a 10^6 Mpc^3 void in Bootes is confirmed by this survey. However, inspection of Figures 1, 3, 4, 5, and 6 reveals a curious point. The void defined by this survey does not appear to extend as far as the three KOSS fields, on the basis of which the original discovery was made. What is to be made of this? It seems to us possible but extremely unlikely that our original velocity gap was unrelated to the void which happened to exist between the three fields. Considerations of probability alone seem to demand that the peculiar density distributions seen in the three KOSS fields be related to the void between them. The most plausible explanation is that the void, although apparently sharply bounded in front and back, is surrounded in other directions by a larger region of low density which the KOSS fields happened to penetrate at particularly empty spots. Unfortunately, our survey area does not extend sufficiently far to test this hypothesis; but the distribution of nearby clusters and superclusters described by Bahcall and Soneira (1982), and a new redshift survey of a region southeast of Bootes (Postman, Geller, and Huchra 1986), suggest that the density structures seen in our galaxy samples may extend over larger angles.

IV. DISCUSSION

a) Theoretical Implications

The general subject of large-scale structure has been reviewed by Oort (1983); Peebles (1984); and Doroshevich, Shandarin, and Zel'dovich (1983). The development of voids has been given explicit theoretical treatment by a number of investigators (for example, Peebles 1982; Sato 1982; Aarseth and Saslaw 1982; Palmer and Voglis 1983; Fujimoto 1983; Hausman, Olson, and Roth 1983; Suto, Sato, and Sato 1984; Fillmore and Goldreich 1985). It is clear that the observed properties of voids can provide significant constraints on cosmological models: constraints which are badly needed, since the most widely used description of the clustering, the galaxy covariance function, appears unable to distinguish between very different clustering scenarios.

The popular models for the growth of clustering in the universe divide roughly into several classes. Gravitational models divide between "bottom up" or hierarchical models, in which structure grows from small to large scales, and "top down" or pancake models, in which large-scale structures form first and then fragment to produce small-scale structure. Examples of the former can be found in the work of Aarseth, Gott, and Turner (1979), and of the latter in Zel'dovich, Einasto, and Shandarin (1982). The cold dark matter model (e.g., Davis *et al.* 1985) is in some ways intermediate between these two classes, with structure forming on a wide range of scales almost simultaneously.

The only widely discussed nongravitational model is the explosive amplification scheme of Ostriker and Cowie (1981). More detailed work by Carr and Ikeuchi (1985), Vishniac, Ostriker, and Bertschinger (1985), and Bertschinger (1985) elaborates these ideas. There is some disagreement over whether this model can produce features as large as the Bootes Void. However, given how poorly much of the relevant astrophysics is understood, this is a rather flexible model which could probably accommodate a wide range of observational facts, and we shall confine further discussion to the better defined gravitational models.

In principle, any of the gravitational models could produce voids of any size. The pancake models would appear particularly favorable for this, because of the cell-like structure of their matter distributions. In practice, however, the observed amplitude of the galaxy covariance function provides a strong constraint on the large-scale structure of any model. We have calculated the probability of finding a void the size of the one in Bootes, using n-body models of four typical clustering scenarios. We take two hierarchical models from West, Dekel, and Oemler (1986). These models assume an initial fluctuation spectrum of the form

$$\langle |\delta_k| \rangle \propto k^n \tag{6}$$

with values of n of 0 and 2. We also use the West *et al.* pancake model, which has a coherence length of $30h^{-1}$ Mpc. Each model contains ~ 4000 particles within a sphere of radius $50h^{-1}$ Mpc. Finally, we use the cold dark matter model of Davis *et al.* (1985); this model contains 32,768 particles in a $128h^{-1}$ Mpc cube. All these models have been evolved and scaled so that the model covariance function matches that observed.

The density of particles in these models is much higher than that of galaxies in our survey. However, as Hamilton (1985) has shown, the probability of finding a void in a sample of a given density may be easily calculated from the statistics of a denser sample. If $P_x(N)$ is the probability of finding x objects in a sphere where the expectation value is N, then

$$P_0(N') = \sum_{x=0}^{\infty} P_x(N)\left(1 - \frac{N'}{N}\right)^x , \tag{7}$$

where $N' < N$. Using $P_x(N)$ calculated from the West *et al.* models and the information in Figure 11 of Davis *et al.* (1985)

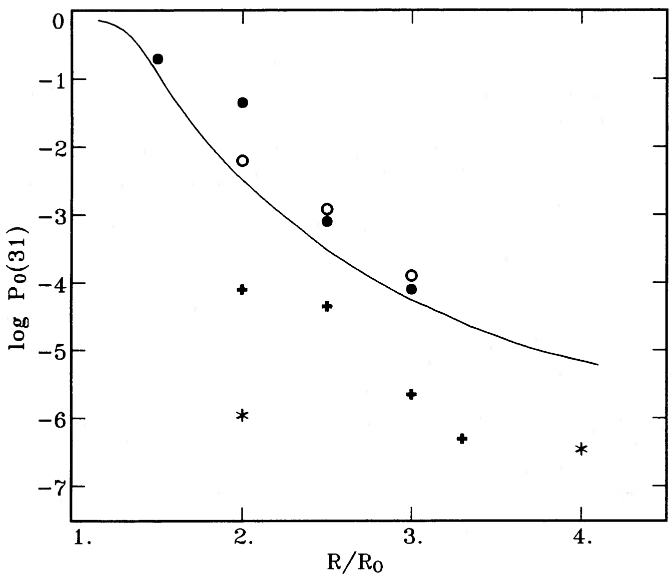

FIG. 7.—Probability of finding a spherical void where 31 galaxies were expected, as a function of the ratio of sphere size to correlation length. *Filled circles*, hierarchical model $n = 0$; *open circles*, hierarchical model $n = 2$; *pluses*, pancake model; *stars*, cold dark matter model; *smooth curve*, Soneira-Peebles model.

for the cold dark matter models, we calculate $P_0(31)$ for voids of various sizes.

The results of our calculations are presented in Figure 7. Since the probability of a spherical void in any model is a function only of the sample density and the ratio of the sphere size R to the correlation length R_0, we plot $P_0(31)$ versus the ratio of those lengths. The radius of our empty sphere is $31h^{-1}$ Mpc. Although the most popular value for the galaxy correlation length is 4–$5h^{-1}$ Mpc, there are strong reasons for preferring a value of $8h^{-1}$ Mpc (Oemler *et al.* 1986). Therefore, a ratio $R/R_0 = 3.8$ corresponds to a void the size of that in Bootes.

Unfortunately, these results are of limited accuracy. Because all the simulations are of volumes not much larger than the Bootes void, and because such a large void is, as can be seen, a quite rare event, the statistical errors in the derived probabilities are quite large. Therefore, as an additional estimate of the void probability, we have calculated $P_0(N)$ in a Soneira-Peebles (1978) analytical model. This model has no physical basis, but it does match both the observed covariance function and the visible appearance of the large-scale distribution of galaxies in the universe. Being an analytical model, it has the advantage that we can easily construct a simulation of sufficiently large volume to minimize the statistical errors. These results are presented in Figure 7 as a smooth curve. All the models give results similar to that from the Soneira-Peebles model and suggest that the probability of finding a void the size of that in Bootes is on the order of 10^{-5}. Even after multiplying this by the factor of 50 which we derived earlier to take account of the number of independent samples available within our survey volume, the Bootes Void remains a very unlikely event in any current scenario.

It appears, then, that most popular cosmological models have difficulty explaining the presence of a void as large as that in Bootes. This may indicate the need for an entirely new theory for the formation of structure in the universe. Alternatively, it may signify that the distribution of matter is substantially different from the distribution of bright galaxies, since it is only the latter that we have determined. The most popular means for producing such an effect is by biased galaxy formation (Kaiser 1984, 1985; Bardeen 1985), in which galaxies form only at the highest density points of the matter distribution. If galaxies do not trace the mass, the Bootes Void may be filled with other forms of matter, and the observational task is to find that material.

b) Contents of the Void

It will be very difficult to rule out all conceivable forms of matter as possible contents of the void, but observations of some forms already exist. Since our observations only determine the distribution of bright, normal galaxies, a logical first candidate would be unusual galaxies. Balzano and Weedman (1982) have examined the spatial distribution of Markarian galaxies with measured redshifts in the direction of Bootes. Using all such galaxies in the region $13^{h}00^{m} < \alpha < 16^{h}05^{m}$, $25° < \delta < 75°$, they found no underabundance of galaxies in the velocity interval of the void. However, because of the large area and limited depth of their sample, the empty region which we have delineated in this survey would have no difficulty hiding within their statistical uncertainties. In fact, Moody (1986) has shown that the Balzano and Weedman sample is consistent with the presence of a substantial void in the velocity interval $12{,}000 < v < 18{,}000$ km s^{-1}. Nevertheless, one of the Markarian galaxies, Mrk 845, is located well within the void.

Sanduleak and Pesch (1982) have used an objective prism on the Burrell Schmidt telescope to search for emission-line galaxies in a $5° \times 26°$ strip that traverses the southern edge of the void at $38° < \delta < 43°$. Tifft *et al.* (1986) have examined spectra of 44 of the objects discovered in this search. Of the 31 objects which were confirmed to be emission-line galaxies, two, Case Galaxy (CG) 1457+42 and CG 1518+39 lie within the void boundaries. Moody (1986) has recently completed a similar survey with the Burrell Schmidt, covering twice the area of the Sanduleak and Pesch survey, and using a plate-filter combination which permitted him to detect galaxies with [O III] emission at greater redshifts. He has found ~50 objects, of which three are within the void. Finally, one additional void galaxy is known, I Zw 81 (Sargent 1970, called in Sargent's paper I Zw 80); it is also a strong emission-line object.[3] All these galaxies are emission-line objects; all but one have strong, high-excitation emission spectra. One, Mrk 845, is a Seyfert I. Strong emission line galaxies are uncommon: for example, they comprise only a few percent of the galaxies in our survey. That these objects have emission lines is, of course, not surprising: the surveys selected for such objects. What is surprising is the abundance of these objects within the void. None of the surveys conducted so far is sufficiently deep or well defined to permit a quantitative comparison of the space distributions of normal and emission-line galaxies. Nevertheless, it is clear that the latter comprise a disproportionate share of those galaxies within the void. Within the same region in which the objective prism surveys have found six of 81 objects to be within the void, we find none of 101. However, although relatively overabundant, it is also clear that their absolute abun-

[3] Since there are objects in this region, our continued use of the word "void" might appear a misnomer. However, since the region is apparently devoid of normal galaxies, we prefer this word over a clumsier if more accurate phrase like "very low density region."

dance is still considerably lower than the cosmic mean. They cannot, therefore, represent the matter which is missing from the normal galaxy population. It may be that these objects will tell us more about the influence of environment on star formation in galaxies than about the large-scale distribution of matter in the universe.

If the formation of galaxies within the void has been inhibited because of some form of biasing, the gas which would normally have formed galaxies should still be present. Hot gas has been searched for by Ceccarelli *et al.* (1983). They scanned the Bootes region in the far-infrared, looking for a change in the temperature of the microwave background caused by Compton scattering of background photons by the gas (Sunyaev and Zel'dovitch 1972). They found no such effect, with a 1 σ upper limit of 1×10^{-4} K. A direct search for soft X-ray emission from hot gas may also be feasible.

If, on the other hand, the void is populated by cold gas clouds, they might be detected in absorption against background sources such as quasars or distant supernovae. One attempt to do this with *IUE* observations has been carried out by Brosch and Gondhalekar (1984). They found weak lines attributable to Lyα, Si IV, and C IV at the void redshift in the spectrum of PG 1351+64 (an object, it should be noted, well to the north of the empty region we have delineated). However, their spectra have low signal-to-noise ratios and unusual line ratios, and better data, presumably requiring Hubble Space Telescope observations, are needed.

We are left, then, with two questions which must be answered if the theoretical implications of this void are to be understood. First, what indeed is the matter content of the void? Second, how common are such large voids? The existence of smaller voids is well documented (Gregory and Thompson 1978; Tarenghi *et al.* 1980). The recent survey of a two-dimensional slice of the universe by de Lapparent, Geller, and Huchra (1986) suggests the existence of other large voids. It should also be noted that the void we have described is not the only one of its size in our survey volume. At least one other exists, at $\alpha = 14^h57^m$, $\delta = +41°$, $cz = 23{,}000$ km s^{-1}. Being more distant, it is of lower significance: only 13 sample galaxies are expected within this volume. All of this suggests that large voids are very common, but it is only suggestive. Much hard work will have to be done before we have a quantitative estimate of their frequency.

We thank Messrs. M. Hanna and G. Pickens for their skilled and patient efforts in the photographic reproduction of the survey fields. This work was partially supported by NSF grant AST81-19986.

APPENDIX

In this Appendix, we expand Politzer and Preskill's (1986, hereafter PP) derivation of void probabilities to include the case of discrete sample fields like those which we have used in Bootes. This discussion assumes familiarity with their paper. PP show that the probability of finding a spherical void of volume v somewhere within a survey volume V is

$$P_{\text{void}} = C(V/v)P_0(N)N^3 , \tag{A1}$$

where N is the mean density of particles per volume v, and C is a constant of order unity. If the particles are uncorrelated, $P_0(N)$ has the Poisson value exp $(-N)$. This equation may be interpreted as follows. $P_0(N)$ is the probability that a given volume v will be empty. The total probability of finding a void is larger than this by a factor equal to the number of independent samples within the survey volume. The sphere volume v is contained within the survey volume V a number V/v times, but the number of independent samples is larger still by a factor N^3. Thus, since we are searching for a void by moving our sphere in three dimensions, we take a new, independent sample each time we move the sphere, in any one of the three orthogonal directions, by an amount equal to L/N, where $L = v^{1/3}$ is the characteristic size of the volume.

Following the reasoning in PP, to which the reader is referred for an explanation of this procedure, we can now calculate an expression analogous to equation (A1) for the case of discrete fields. Since the spacing of fields is discrete only in the two coordinates on the plane of the sky, we do the calculation in two dimensions. We assume the distribution of fields shown in Figure 8. For convenience, we use a rectangular rather than a circular area; PP show that this makes little difference, as long as the orientation of the square is fixed. The square has length L and the spacing of fields is l. The mean particle density per field is n. We can, with little loss of generality, assume that L/l is an integer, in which case we can also assume that squares are always centered on a field, since all intermediate positions will contain the same fields. Clearly, the chance of a particular square being empty

$$P(0) = P_0[n(L/l)^2] , \tag{A2}$$

and the number of empty squares per unit area

$$\rho_0 = P_0[n(L/l)^2]/l^2 . \tag{A3}$$

The fraction of such empty squares which are also first encounters (see PP) is approximately equal to the probability that a particular square has one or more particles in each of the areas A and B. Now, in A,

$$\begin{aligned} P(N > 0) &= P_{>0}[n(L/l)] \\ &= 1 - P_0[n(L/l)] , \end{aligned} \tag{A4}$$

so the fraction of first encounters is just $\{1 - P_0[n(L/l)]\}^2$. Therefore, the total number of distinct voids per unit area is just

$$\rho_0 = P_0(N)\{1 - P_0[n(L/l)]\}^2/l^2 , \tag{A5}$$

and the number per square is just

$$N = P_0(N)(L/l)^2\{1 - P_0[n(L/l)]\}^2 , \tag{A6}$$

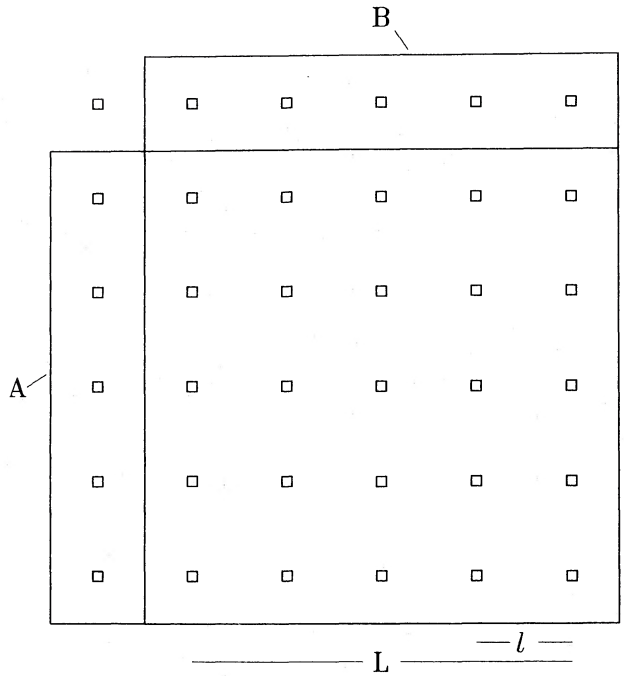

FIG. 8.—Layout of fields for calculation of void probability

where $N = n(L/l)^2$ is the mean expected number of particles per square. If the particles are uncorrelated,

$$N = P_0(N)(L/l)^2\{1 - \exp[n(L/l)]\}^2 . \tag{A7}$$

If $n(L/l) \gg 1$, which is almost true of our sample, then

$$N \propto P_0(N)(L/l)^2 , \tag{A8}$$

in which case we obtain an independent sample whenever we move the square by a distance l. This seems obvious, but note that it is only true in the limit of high density.

It follows, then, from equations (A1) and (A8) that the number of independent samples which we have searched to find our spherical void is just equal to the number of positions within our survey volume at which we can center a $R = 62$ Mpc sphere, spacing positions in right ascension and declination by the distance between survey fields, and in distance by R/N, where N is the number of independent groups, 17.5.

REFERENCES

Aarseth, S. J., Gott, J. R., and Turner, E. L. 1979, *Ap. J.*, **228**, 664.
Aarseth, S. J., and Saslaw, W. C. 1982, *Ap. J. (Letters)*, **258**, L7.
Bahcall, N. A., and Soneira, R. M. 1982, *Ap. J. (Letters)*, **258**, L17.
Balzano, V. A., and Weedman, D. W. 1982, *Ap. J. (Letters)*, **255**, L1.
Bardeen, J. 1985, in *Inner Space/Outer Space*, ed. E. W. Kolb, M. S. Turner, D. Lindley, K. Olive, and D. Sekel (Chicago: University of Chicago Press), p. 212.
Bertschinger, E. 1985, *Ap. J.*, **295**, 1.
Brosch, N., and Gondhalekar, P. M. 1984, *Astr. Ap.*, **140**, L43.
Carr, B. J., and Ikeuchi, S. 1985, *M.N.R.A.S.*, **213**, 497.
Ceccarelli, C., Melchiorri, F., Pietranera, L., Dall'Oglio, G., and Melchiorri, B. O. 1983, *Nature*, **305**, 196.
Davis, M., Efstathiou, G., Frenk, C. S., and White, S. D. M. 1983, *Ap. J.*, **292**, 371.
de Lapparent, V., Geller, M. J., and Huchra, J. P. 1986, *Ap. J. (Letters)*, **302**, L1.
de Vaucouleurs, G., de Vaucouleurs, A., and Corwin, H. G. 1976, *Second Reference Catalogue of Bright Galaxies* (Austin: University of Texas Press) (RC2).
Doroshevich, A. G., Shandarin, S. F., and Zel'dovich, Y. A. 1983, in *IAU Symposium 104, Early Evolution of the Universe And Its Present Structure*, ed. G. O. Abell and G. Chincarini (Dordrecht: Reidel), p. 387.
Fillmore, J. A., and Goldreich, P. 1985, *Ap. J.*, **281**, 9.
Fujimoto, M. 1983, *Pub. Astr. Soc. Japan*, **35**, 159.
Gregory, S. A., and Thompson, L. A. 1978, *Ap. J.*, **222**, 784.
Hamilton, A. J. S. 1985, *Ap. J. (Letters)*, **292**, L25.
Hausman, M. A., Olson, D. W., and Roth, B. D. 1983, *Ap. J.*, **270**, 351.
Huchra, J., Davis, M., Latham, D., and Tonry, J. 1983, *Ap. J. Suppl.*, **52**, 89.
Kaiser, N. 1984, *Ap. J. (Letters)*, **284**, L9.
Kaiser, N. 1985, in *Inner Space/Outer Space*, ed. E. W. Kolb, M. S. Turner, D. Lindley, K. Olive, and D. Sekel (Chicago: University of Chicago Press), p. 258.
Kirshner, R. P., Oemler, A., and Schechter, P. L. 1978, *A.J.*, **83**, 1589.
———. 1979, *A.J.*, **84**, 951.
Kirshner, R. P., Oemler, A., Schechter, P. L., and Shectman, S. A. 1981, *Ap. J. (Letters)*, **248**, L57.
———. 1983*a*, *A.J.*, **88**, 1285. (KOSS).
———. 1983*b*, in *IAU Symposium 104, Early Evolution of the Universe and Its Present Structure*, ed. G. O. Abell and G. Chincarini (Dordrecht: Reidel), p. 197.
———. 1984, in *Eleventh Texas Symposium on Relativistic Astrophysics*, ed. D. S. Evans (Ann. NY Acad. Sci., Vol. **422**), p. 91.
Moody, J. W. 1986, Ph.D. thesis, University of Michigan.
Oemler, A., Shechter, P. L., Shectman, S. A., and Kirshner, R. P. 1986, in preparation.
Oort, J. 1983, *Ann. Rev. Astr. Ap.*, **21**, 373.
Ostriker, J. P., and Cowie, L. L. 1981, *Ap. J. (Letters)*, **243**, L127.
Palmer, P. L., and Voglis, N. 1983, *M.N.R.A.S.*, **205**, 543.
Peebles, P. J. E. 1982, *Ap. J.*, **257**, 438.
———. 1984, *Science*, **224**, 1385.
Politzer, H. D., and Preskill, J. P. 1986, *Phys. Rev. Letters*, **56**, 99.
Postman, M., Geller, M., and Huchra, J. B. 1986, *A.J.*, in press.
Sanduleak, N., and Pesch, P. 1982, *Ap. J. (Letters)*, **258**, L11.
Sargent, W. L. W. 1970, *Ap. J.*, **160**, 405.
Sato, H. 1982, *Progr. Theor. Phys.*, **68**, 236.
Schechter, P. L. 1976, *Ap. J.*, **203** 297.
Soneira, R. M., and Peebles, P. J. E. 1978, *A.J.*, **83**, 845.

Sunyaev, R. A., and Zel'dovich, Ya. B. 1972, *Comm. Ap. Space Sci.*, **14**, 173.
Suto, Y., Sato, K., and Sato, H. 1984, *Progr. Theor. Phys.*, **71**, 938.
Tarenghi, M., Chincarini, G., Rood, N. J., and Thompson, L. A. 1980, *Ap. J.*, **235**, 724.
Tifft, W. G., Kirshner, R. P., Gregory, S. A., and Moody, J. W. 1986, *Ap. J.*, **310**, 75.
West, M. J., Dekel, A., and Oemler, A. 1986, in preparation.
Vishniac, E., Ostriker, J. P., and Bertschinger, E. 1985, *Ap. J.*, **291**, 399.
Zel'dovich, Ya. B., Einasto, H., and Shandarin, S. F. 1982, *Nature*, **300**, 407.

ROBERT P. KIRSHNER: Center for Astrophysics, 60 Garden St., Cambridge, MA 29928

AUGUSTUS OEMLER, JR.: Department of Astronomy, Yale University, P.O. Box 6666, New Haven, CT 06511

PAUL L. SCHECHTER and STEPHEN A. SHECTMAN: Mount Wilson and Las Campanas Observatories, 813 Santa Barbara St., Pasadena, CA 91101